Conference materials
UDC 535.42
DOI: https://doi.org/10.18721/JPM.173.146

Optical needle formation by subwavelength optical elements using high-performance computer systems

D.A. Savelyev [1] ✉

[1] Samara National Research University, Samara, Russia
✉ dmitrey.savelyev@yandex.ru

Abstract. The optical vortex diffraction on subwavelength optical elements with a standard and GRIN substrate using the finite difference time domain method was simulated in this paper. The possibility of increasing the light needle (up to 7.86λ) for input radiation with azimuthal and radial polarization was shown using a GRIN substrate and a subwavelength element with zones alternating in height.

Keywords: optical vortices, GRIN, subwavelength ring gratings, FDTD

Funding: This research was funded by the Russian Science Foundation (project No. 24-22-00044), https://rscf.ru/en/project/24-22-00044/.

Citation: Savelyev D.A., Optical needle formation by subwavelength optical elements using high-performance computer systems, St. Petersburg State Polytechnical University Journal. Physics and Mathematics. 17 (3.1) (2024) 229–232. DOI: https://doi.org/10.18721/JPM.173.146

Материалы конференции
УДК 535.42
DOI: https://doi.org/10.18721/JPM.173.146

Формирование оптических игл субволновыми оптическими элементами с использованием высокопроизводительных компьютерных систем

Д.А. Савельев 1✉

[1] Самарский национальный исследовательский университет им. академика С.П. Королева, г. Самара, Россия
✉ dmitrey.savelyev@yandex.ru

Аннотация. В работе методом конечных разностей во временной области проведено моделирование дифракции оптических вихрей на субволновых оптических элементах со стандартной и GRIN-подложкой. Показана возможность увеличения фокального светового отрезка для азимутальной и радиальной поляризации входного излучения при использовании GRIN-подложки и субволнового элемента с чередующимися по высоте зонами.

Ключевые слова: оптические вихри, GRIN, субволновые кольцевые решетки, FDTD

Финансирование: Работа выполнена при финансовой поддержке Российского научного фонда (проект № 24-22-00044, https://rscf.ru/project/24-22-00044/).

Ссылка при цитировании: Савельев Д.А. Формирование оптических игл субволновыми оптическими элементами с использованием высокопроизводительных компьютерных систем // Научно-технические ведомости СПбГПУ.

Физико-математические науки. 2024. Т. 17. № 3.1. С. 229–232. DOI: https://doi.org/10.18721/JPM.173.146

Introduction

Optical vortices are known for their use in various applications [1–5], among which are optical manipulation [2], sensing, optical information transmission, and sharp focusing [3, 5, 6]. Some optical structures can be used to generate optical vortices such as spiral phase plates [7], metasurfaces, and ring gratings [1, 6]. The ring gratings and diffraction axicons in various combinations are also used to obtain optical needles with a large depth of focus [6, 8].

Also currently well known is the use of materials with a gradient refractive index (GRadient Index, GRIN) to control the propagation of light, solve problems of optical communication, and light collimation [6, 9], in biology [10].

Thus, the study of the diffraction of Laguerre-Gaussian modes (optical vortices) on subwavelength ring gratings with a GRIN substrate was carried out in this paper to form an elongated focal segment (light needle).

Materials and Methods

The numerical simulations (3D) were carried out using the finite difference time domain (FDTD) method on an 900 Gflop computing cluster with using Meep software package [11]. This modeling parameters were considered: the wavelength λ of the input radiation was equal to 0.532 μm, space step – $\lambda/35$, time step – $\lambda/(70c)$, where c is the speed of light. The size of the three-dimensional computational domain is $15.8\,\lambda$. The computational region was surrounded on all sides by an absorbing layer PML (with size $1.12\,\lambda$). The Laguerre-Gauss mode (1,0) (optical vortices of the first order, $\sigma = 1.5$ μm) with radial and azimuthal polarization were considered as input radiation.

The variable-height ring gratings with a standard substrate (refractive index $n = 1.47$) and a GRIN substrate were considered. The refractive index of GRIN substrate was varied uniformly from the maximum refractive index in the center ($n = 2.7$) to the minimum refractive index at the edges ($n = 1.47$). The GRIN substrate consisted of rings of the same width.

The refractive index of the relief was $n = 1.47$. The relief height of the elements h was chosen based on the phase jump π radians, respectively, for $n = 1.47$ the base height h was $1.06\,\lambda$ (π). Next, the height of the odd (h_1) and even (h_2) relief zones of the elements was varied, also based on the phase jump π radians.

The production of such elements seems possible, since the possibility of producing a relief of optical elements with an aspect ratio of more than 1000 was previously shown [12].

Results and Discussion

The length of the light segment was estimated by the full length by the half maximum of the radiation intensity (DOF), similarly to the assessment of the focal spot on the optical axis – by the full width at half maximum (FWHM) of the intensity.

A diffraction axicon with a height of $h = 1.06\,\lambda$ (Fig. 1, *c*) with a standard substrate acted as a basic optical element for comparison. Increasing the height of the relief, as well as the use of a GRIN substrate, made it possible to increase the length of the light needle. Separately, cases were assessed when the height h1 was fixed ($1.06\,\lambda$) and the height h_2 changed (Fig. 2) and the reverse case (Fig. 3).

It should be noted that an increase in height led to the formation of a powerful light needle for radial polarization, in contrast to the case of the same polarization for a standart axicon with a height $h_1 = 1.06\,\lambda$ (a minimum on the optical axis and the formation of a ring were observed).

The maximum light needle size was obtained for radial polarization at $h_1 = 5.32\,\lambda$, $h_2 = 1.06\,\lambda$ (DOF = $7.86\,\lambda$), which is 3.19 times longer than in the case of the basic optical element.

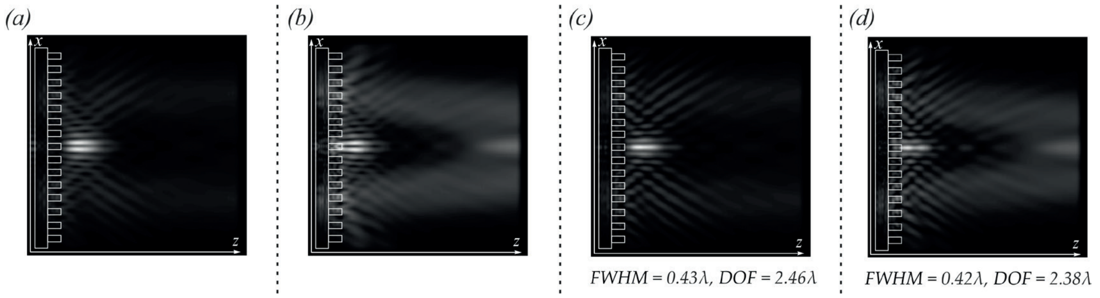

(c) FWHM = 0.43λ, DOF = 2.46λ

(d) FWHM = 0.42λ, DOF = 2.38λ

Fig. 1. The two-dimensional diffraction pattern (*xz* plane) of an optical vortex on ring gratings (total intensity), with relief height $h = 1.06\,\lambda$, radial polarization and (*a*) standard substrate, (*b*) GRIN substrate; azimuthal polarization and (*c*) standard substrate, (*d*) GRIN substrate

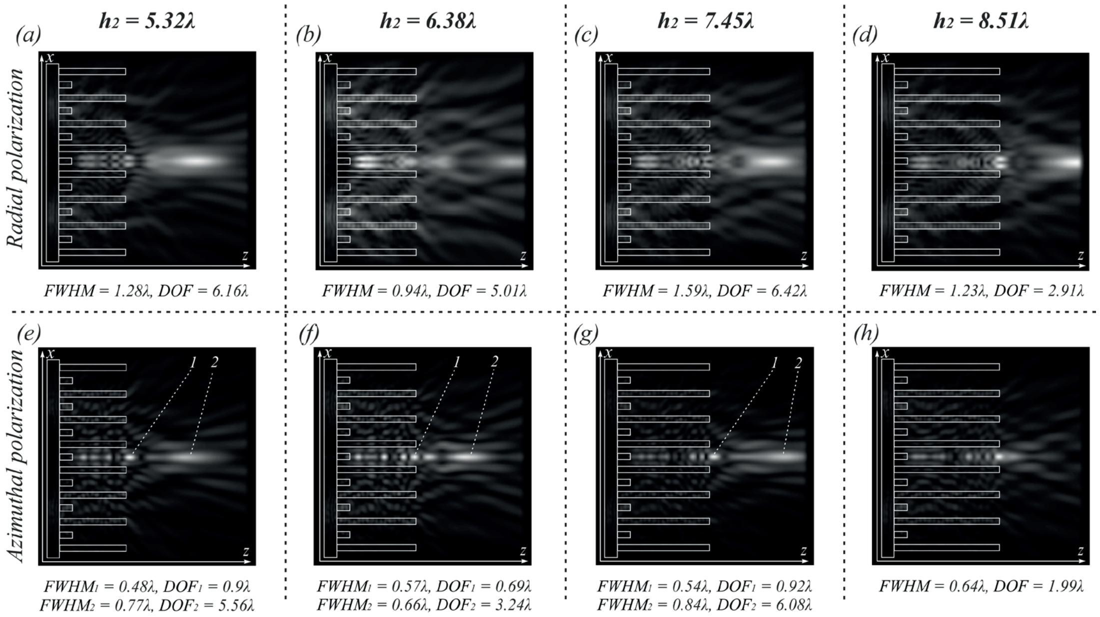

(a) h2 = 5.32λ — FWHM = 1.28λ, DOF = 6.16λ

(b) h2 = 6.38λ — FWHM = 0.94λ, DOF = 5.01λ

(c) h2 = 7.45λ — FWHM = 1.59λ, DOF = 6.42λ

(d) h2 = 8.51λ — FWHM = 1.23λ, DOF = 2.91λ

(e) FWHM1 = 0.48λ, DOF1 = 0.9λ
FWHM2 = 0.77λ, DOF2 = 5.56λ

(f) FWHM1 = 0.57λ, DOF1 = 0.69λ
FWHM2 = 0.66λ, DOF2 = 3.24λ

(g) FWHM1 = 0.54λ, DOF1 = 0.92λ
FWHM2 = 0.84λ, DOF2 = 6.08λ

(h) FWHM = 0.64λ, DOF = 1.99λ

Fig. 2. The two-dimensional diffraction pattern (*xz* plane) of an optical vortex on ring gratings (total intensity, for fixed $h_1 = 1.06\,\lambda$), with radial polarization (*a*, *b*, *c*, *d*) and azimuthal polarization (*e*, *f*, *g*, *h*)

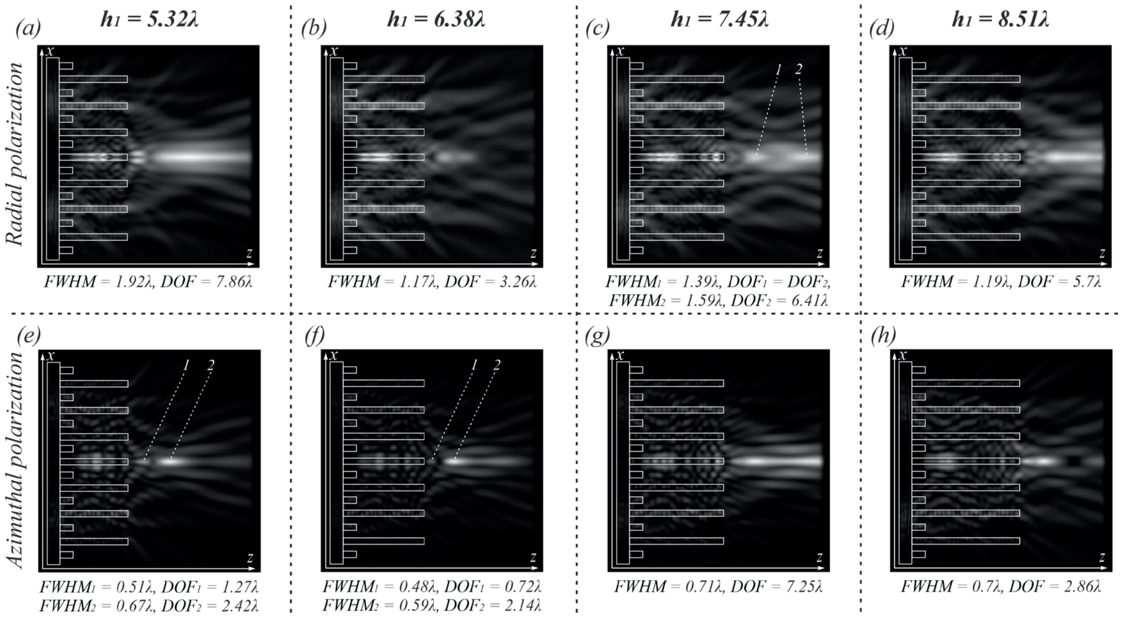

(a) h1 = 5.32λ — FWHM = 1.92λ, DOF = 7.86λ

(b) h1 = 6.38λ — FWHM = 1.17λ, DOF = 3.26λ

(c) h1 = 7.45λ — FWHM1 = 1.39λ, DOF1 = DOF2,
FWHM2 = 1.59λ, DOF2 = 6.41λ

(d) h1 = 8.51λ — FWHM = 1.19λ, DOF = 5.7λ

(e) FWHM1 = 0.51λ, DOF1 = 1.27λ
FWHM2 = 0.67λ, DOF2 = 2.42λ

(f) FWHM1 = 0.48λ, DOF1 = 0.72λ
FWHM2 = 0.59λ, DOF2 = 2.14λ

(g) FWHM = 0.71λ, DOF = 7.25λ

(h) FWHM = 0.7λ, DOF = 2.86λ

Fig. 3. The two-dimensional diffraction pattern (*xz* plane) of an optical vortex on ring gratings (total intensity, for fixed $h_2 = 1.06\,\lambda$), with radial polarization (*a*, *b*, *c*, *d*) and azimuthal polarization (*e*, *f*, *g*, *h*)

And for azimuthal polarization, the maximum size of the light segment was obtained for $h_1 = 5.32\,\lambda$, $h_2 = 1.06\,\lambda$ (DOF = 7.25 λ). An increase in the size of the light segments is accompanied by an increase in the size of the focal spots.

It should also be noted that for a number of cases considered, a set of maxima is formed on the optical axis (especially noticeable for azimuthal polarization at a fixed h_1 =1.06). The intensity oscillations on the optical axis were observed inside the element for the case with fixed h_2.

Conclusion

The diffraction of first-order optical vortices with azimuthal and radial polarization on subwavelength ring gratings of variable height with a GRIN substrate using the FDTD method was simulated in this paper.

The maximum light needle on the optical axis (DOF = 7.86 λ) was obtained for an element with alternating zones ($h_1 = 5.32\,\lambda$, $h_2 = 1.06\,\lambda$) with radial polarization of input radiation.

REFERENCES

1. **Shen Y., Wang X., Xie Z., Min C., Fu X., Liu Q., Gong M., Yuan X.,** Optical vortices 30 years on: OAM manipulation from topological charge to multiple singularities, Light: Science & Applications. 8 (1) (2019) 1–29.
2. **Wen, J., Gao, B., Zhu, G., Liu, D., Wang, L.G.,** Precise position and angular control of optical trapping and manipulation via a single vortex-pair beam, Optics and Lasers in Engineering. 148 (2022) 106773.
3. **Dong M., Zhao C., Cai Y., Yang Y.,** Partially coherent vortex beams: Fundamentals and applications, Science China Physics, Mechanics & Astronomy. 64 (2) (2021) 224201.
4. **Khonina S.N.,** Vortex beams with high-order cylindrical polarization: features of focal distributions, Applied Physics B. 125 (6) (2019) 100.
5. **Savelyev D.A.,** Features of a Gaussian beam near-field diffraction upon variations in the relief height of subwavelength silicon optical elements, Computer Optics. 47 (6) (2023) 938–947.
6. **Savelyev D.A., Karpeev S.V.,** Development of 3D Microstructures for the Formation of a Set of Optical Traps on the Optical Axis, Photonics. 10 (2) (2023) 117.
7. **Lightman S., Hurvitz G., Gvishi R., Arie A.,** Miniature wide-spectrum mode sorter for vortex beams produced by 3D laser printing, Optica. 4 (6) (2017) 605–610.
8. **Shi C., Xu Z., Nie Z., Xia Z., Dong B., Liu J.,** Sub-wavelength longitudinally polarized optical needle arrays generated with tightly focused radially polarized Gaussian beam, Optics communications. 505 (2022) 127506.
9. **Richardson K.A., Kang M., Sisken L., Yadav A., Novak S., Lepicard A., Martin I., Francois-Saint-Cyr H., Schwarz C.M., Mayer T.S., Rivero-Baleine C., Yee A. J., Mingareev I.,** Advances in infrared gradient refractive index (GRIN) materials: a review, Optical Engineering. 59 (11) (2020) 112602.
10. **Guo C., Urner T., Jia S.,** 3D light-field endoscopic imaging using a GRIN lens array, Applied Physics Letters. 116 (10) (2020) 101105.
11. **Srivastava P.R., Majumdar A., Menon R., Swartzlander G.A.,** High forward thrust metasurface beam-riding sail, Optics Express. 32 (2) (2024) 1756–1763.
12. **Zhang L., Jiang F., Wu B., Lv C., Wu M.,** A one-step synthesis of ultra-long silver nanowires with ultra-high aspect ratio above 2000 and its application in flexible transparent conductive electrodes, Nanotechnology. 32 (10) (2020) 105710.

THE AUTHORS

SAVELYEV Dmitry A.
dmitrey.savelyev@yandex.ru
ORCID: 0000-0003-2282-3895

Received 06.07.2024. Approved after reviewing 01.08.2024. Accepted 03.08.2024.